Electronic and Steric Control of the Formation of C-H-M from M-H-M Interactions in Carbon Atom Capped Transition-Metal Carbonyl Clusters. Effect of the Metal Fragment

Reynaldo D. Barreto, Jose Puga, and Thomas P. Fehlner*

Department of Chemistry, University of Notre Dame, Notre Dame, Indiana 46556

Received July 18, 1989

The carbon-capped triangular trimetal cluster with the composition $FeCo_2(CO)_9(CHR)$ exists in solution as an equilibrium mixture of two tautomers: $HFeCo_2(CO)_9(CR)$ [I] = $FeCo_2(CO)_9(HCR)$ [II]; R = Me, Ph, 3-PhC_6H_4, 3-*t*-BuC_6H_4, β-naphthyl, and 2,3-$Me_2C_6H_3$. The equilibrium constants have been measured by NMR and/or IR methods, while the rate constants for the interconversion of I and II have been obtained by line-shape analysis of the NMR data. Variable-temperature IR spectroscopy has been used to define the temperature dependence of the equilibrium ratio for R = Ph. Although the energy difference between tautomers is small, an analysis of the spectroscopic data for both species shows that the bonding of both the hydrocarbyl fragment and the metal carbonyl fragment change substantially, but in a complementary manner, in going from I to II. The data demonstrate that the substituent on the carbyne carbon can perturb the equilibrium via a steric effect; however, the importance of electronic effects on the equilibrium constant is evident in the comparison of the mixed-metal system with other isoelectronic clusters.

The reaction of main-group atoms and fragments, particularly those containing carbon, with hydrogen in the presence of a transition metal is one of the most important and well-studied chemical processes in chemistry.[1] The approaches used to investigate this chemistry range from the direct to the indirect. Among the latter, the metal cluster–metal surface analogy, which draws attention to the similarity in the properties of a ligand bound in a discrete transition-metal cluster to those of a ligand bound to a site on a metal surface, has generated considerable interest.[2] Most comparisons of this type have been made on a structural level and provide descriptions of stable bonding modes. Information on reactivity, however, is crucial as stable structures, even if found in both discrete clusters and on metal surfaces, may not lie on the reaction pathway, i.e., "dead-end" complexes are aptly named.[3] The use of the cluster–surface analogy for reactivity comparisons is difficult simply because, by definition, catalytically important species are found in potential energy wells of similar energy connected by low barriers. Hence, a single cluster model yields little information pertinent to reactivity. However, there are a number of cluster systems known that undergo rapid and often complex structural interconversions.[4] The kinetic and equilibrium properties of such systems provide a means of applying the cluster–surface hypothesis to a reaction type such as hydrogen transfer.

Recently, we have explored main-group-atom-capped trimetal cluster systems in which tautomers, differing only in the number of M-H-M and M-H-C (agostic) interactions,[5] exist in equilibrium with each other. These types of systems have been known for some time beginning with the elegant work of Shapley and co-workers,[6] and agostic hydrogens have been identified as features of important intermediates in the reactions of carbon-capped trinuclear transition-metal clusters.[7] We have emphasized comparisons of hydrocarbyl systems with the isoelectronic ferraborane clusters[8] and have demonstrated spontaneous formation of an agostic hydrogen on deprotonation of a triiron methylidyne cluster.[9] The equilibrium constants for such tautomerizations were thus shown to be very sensitive to the identity of the main-group atom among other things. To permit greater utilization of the cluster–surface analogy in understanding a fundamental reaction type, further definition of the factors that affect the transfer of hydrogen to and from the main-group atom is necessary. An unanswered question is the sensitivity of such an equilibrium to metal identity.

The cluster having the composition $FeCo_2(CO)_9(CHR)$ is isoelectronic to the cluster $Fe_3(CO)_9(CH_3R)$, which exists in solution as a mixture of three tautomers containing zero, one, and two C-H-Fe agostic interactions.[10] Comparison of this system with the isoelectronic ferraborane[8] as well as with heavier congeners[11] suggests that $FeCo_2(CO)_9$(CHR) should exhibit a greater tendency for the formation of C-H-M interactions than $Fe_3(CO)_9(CH_3R)$. $FeCo_2$-$(CO)_9$(CHR) was first prepared by Geoffroy et al. during a pioneering study on the synthesis of mixed-metal clusters.[12] On the basis of room-temperature NMR spectra and the conventional structural wisdom of the time, the single endo hydrogen was assigned a position associated with the trimetal framework. More recently a crystallographic study of the phenyl derivative has appeared.[13] Although the endo hydrogen was not located, relative M-M distances and the crystallographically characterized

(1) See, for example: Gates, B. C.; Guczi, L.; Knözinger, H. *Metal Clusters in Catlaysis*; Elsevier: Amsterdam, 1986.
(2) See, for example: Muetterties, E. L. *Chem. Soc. Rev.* **1982**, *11*, 283.
(3) Beebe, T. P., Jr.; Yates, J. T., Jr. *J. Am. Chem. Soc.* **1986**, *108*, 663.
(4) See, for example: Kolis, J. W.; Holt, E. M.; Shriver, D. F. *J. Am. Chem. Soc.* **1983**, *105*, 7307. Horwitz, C. P.; Shriver, D. F. *J. Am. Chem. Soc.* **1985**, *107*, 8147.
(5) Brookhart, M.; Green, M. L. H. *J. Organomet. Chem.* **1983**, *250*, 395. Crabtree, R. H. *Chem. Rev.* **1985**, *85*, 245. Brookhart, M.; Green, M. L. H.; Wong, L.-L. *Prog. Inorg. Chem.* **1988**, *36*, 1.
(6) Calvert, R. B.; Shapley, J. R. *J. Am. Chem. Soc.* **1977**, *99*, 5225. Calvert, R. B.; Shapley, J. R.; Schultz, A. J.; Williams, J. M.; Suib, S. L.; Stucky, G. D. *J. Am. Chem. Soc.* **1978**, *100*, 6240. Calvert, R. B.; Shapley, J. R. *Ibid.* **1978**, *100*, 7726. Cowie, A. G.; Johnson, B. F. G.; Lewis, J. R.; Raithby, P. R. *J. Organomet. Chem.* **1986**, *306*, C63. Hriljzc, J. A.; Harris, S.; Shriver, D. F. *Inorg. Chem.* **1988**, *27*, 816.
(7) Dugan, T. P.; Barnett, D. J.; Muscatella, M. J.; Keister, J. B. *J. Am. Chem. Soc.* **1986**, *108*, 6076. Bower, D. K.; Keister, J. B. *J. Organomet. Chem.* **1986**, *312*, C33. Van der Velde, D. G.; Holmgren, J. S.; Shapley, J. R. *Inorg. Chem.* **1987**, *26*, 3077.
(8) Vites, J. C.; Housecroft, C. E.; Eigenbrot, C.; Buhl, M. L.; Long, G. J.; Fehlner, T. P. *J. Am. Chem. Soc.* **1986**, *108*, 3304.
(9) Vites, J. C.; Jacobsen, G.; Dutta, T. K.; Fehlner, T. P. *J. Am. Chem. Soc.* **1985**, *107*, 5563.
(10) Dutta, T. K.; Vites, J. C.; Jacobsen, G. B.; Fehlner, T. P. *Organometallics* **1987**, *6*, 842.
(11) Only a single species, $(\mu\text{-H})_3M_3(CO)_9CH$, is observed for M = Ru, Os: Eady, C. R.; Johnson, B. F. G.; Lewis, J. *J. Chem. Soc., Dalton, Trans.* **1977**, 477. Deeming, A. J.; Underhill, M. *J. Chem. Soc., Chem. Commun.* **1977**, 277.
(12) Epstein, R. A.; Withers, H. W.; Geoffroy, G. L. *Inorg. Chem.* **1979**, *18*, 942.
(13) Ahlgren, M.; Pakkanen, T. T.; Tahvanainen, I. *J. Organomet. Chem.* **1987**, *323*, 91.

0276-7333/90/2309-0662$02.50/0

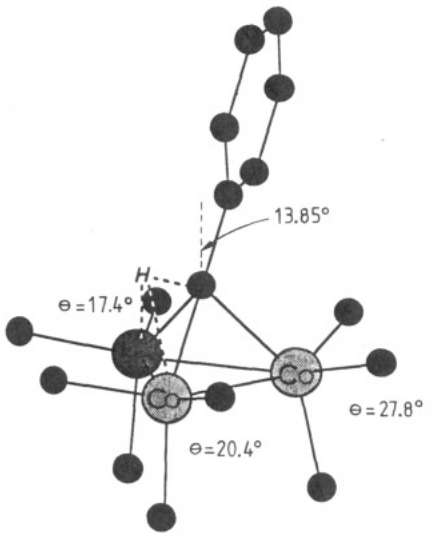

Figure 1. Representation of the crystallographic results of ref 13. The "tilt" angles Θ are defined in ref 15. The geometrical data are best fit by placement of the bridging hydrogen on the FeCoC face as shown.

M–M bridging position of the isolobal $AuPPh_3$ derivative led these authors to suggest a M–M bridging position for the hydride. The conflict between the interpretation of our work on closely related clusters and these structural assignments caused us to reexamine the $FeCo_2(CO)_9(CHR)$ system in more detail.[14] The results demonstrated that the $FeCo_2(CO)_9(CHR)$ cluster system also exists in solution as a mixture of two tautomers.

In the following the complete characterization of the behavior of $FeCo_2(CO)_9(CHR)$ in solution is reported, and the observed tautomeric equilibrium is used to explore an alkyne-to-alkene interconversion on a mixed trimetal site. The roles of the substituent on the capping carbon and the nature of the transition metals are thereby defined precisely by the magnitudes of the rate and equilibrium constants relating alkyne complex to alkene complex. A correlation of the change in equilibrium constant with atom or fragment properties yields insight into the interactions important in providing the driving forces for alkyne to alkene interconversion.

Structural Forms of $FeCo_2(CO)_9(CHR)$

Geometric Analysis of $FeCo_2(CO)_9(CHR)$. An analysis of the spatial distribution of the terminal carbonyls in main-group-atom-capped trimetal clusters as a function of the number of endo hydrogens allowed us to develop a simple correlation between the "tilt" (Θ) of the CO's with respect to the trimetal plane plus the "twist" of the CO's with respect to the pseudo-C_3 axis and the number and position of the bridging hydrogens.[15] Pertinent to this problem is the conclusion that M–M bridging makes Θ larger than 29.8° (the value in a cluster with no endo hydrogens and a first-row capping atom) while M–E bridging (E = main-group atom) makes Θ smaller. These qualitative changes are observed for clusters with one, two, and three endo hydrogens. As shown on the representation of the solid-state structure of $FeCo_2(CO)_9(CHR)$ in Figure 1, one metal center has Θ = 27.8 (3)°, which is near that expected for an unbridged site, while the Θ values of the other two metal sites, 17.4 (3) and 20.4 (4)°, are considerably *smaller*. This suggests the single endo hydrogen is associated with M–C rather than M–M bridging. Finally, the phenyl substituent is bent away from the M_2E face containing the metals with low "tilt" angles. These structural distortions suggest that the cluster contains either a M–C edge or M_2C face bridging rather than a M–M edge or M_3 face bridging endo hydrogen. Nonzero "twist" angles for the latter metal centers corroborate the interaction of the endo hydrogen with this face of the cluster.[16]

Chart I

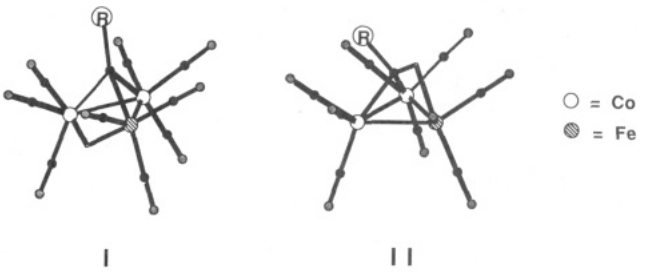

I II

Selective Labeling and NMR Study. To demonstrate that the endo hydrogen interacts with the capping carbon, we prepared $FeCo_2(CO)_9(*CHPh)$ with >98% ^{13}C in the capping atom position using known reactions. Despite having only one endo-hydrogen atom, the low-temperature ^1H NMR spectrum of $FeCo_2(CO)_9(*CHPh)$ exhibited two signals in the hydride region. The doublet at $\delta = -8.23$ ($J_{CH} = 59$ Hz) with relative intensity 2 has a chemical shift and ^{13}C–^1H coupling constant characteristic of a C–H–Fe agostic proton,[5] while the singlet at δ −17.81 with relative intensity 1 has a chemical shift appropriate to a M–M bridging proton.[17] In agreement with the proton data, the ^{13}C NMR spectrum at low temperature showed a singlet at $\delta = 281.4$ of relative intensity 1 and a doublet at 189.4 ($J_{CH} = 59.8$ Hz) of relative intensity 1.7 that collapses to a singlet on proton decoupling. The low-field chemical shift of the singlet is characteristic of a μ_3-carbyne carbon, while the much higher field shift of the doublet is characteristic of a metal-bridging carbene.[18] Clearly this cluster exists in solution as an equilibrium mixture of two tautomers as in reaction 1 and Chart I (R = Ph). The ^1H

$$\underset{\text{I}}{HFeCo_2(CO)_9(CR)} = \underset{\text{II}}{FeCo_2(CO)_9(HCR)} \qquad (1)$$

signal at δ −17.81 can be due to either Fe–Co or Co–Co bridging protons, but I undoubtedly has one of the structures suggested for $FeCo_2(CO)_9(CHPh)$ by the earlier workers.[12,13] On the other hand, the more abundant species in solution at low temperature is the one containing a C–M bridging hydrogen. The question of face vs edge bridging and the particular face or edge that is bridged is not resolved by the NMR data and is discussed further below. The finite ^{13}C–^1H coupling constant proves that the endo hydrogen in tautomer II is associated with the main-group-capping atom while the relatively small magnitude of this coupling constant also demonstrates a relatively strong interaction of this hydrogen with a metal atom.

Infrared Study. In Figure 2 the IR spectra of the phenyl derivative in the carbonyl stretching region is presented. The spectrum is the same as that published earlier.[12] Previously the spectrum was attributed to a single species, but we have now been able to assign some

(14) A preliminary report has appeared: Barreto, R. D.; Fehlner, T. P. *J. Am. Chem. Soc.* **1988**, *110*, 4471.
(15) Lynam, M. M.; Chipman, D. M.; Barreto, R. D.; Fehlner, T. P. *Organometallics* **1987**, *6*, 2405.
(16) Barreto, R. D. Ph.D. Thesis, University of Notre Dame, 1988.
(17) The spectra appear in the original communication, and a spectrum of the unlabeled compound is shown in Figure 3.
(18) Herrmann, W. A. *Adv. Organomet. Chem.* **1982**, *20*, 209.

Table I. Infrared Frequencies in the CO Region for $FeCo_2(CO)_9(CHR)$[a]

assgnt[b]	Me	Ph	3-PhC_6H_4	t-BuC_6H_4	β-napth	2,3-$Me_2C_6H_3$
I	2106 sh	2105 mw	2107 mw	2106 mw	2107 mw	2108 mw
II	2100 m	2099 m	2100 m	2099 m	2100 m	2102 m
I	2064 sh	2064 ms	2068 ms	2064 ms	2066 ms	2069 ms
II and I[c]	2052 vs	2054 vs	2055 vs	2057 vs	2055 vs	2058 vs
I and/or II	2045 vs	2045 s	2047 vs	2048 vs	2048 vs	2049 vs
I and/or II	2038 s	2038 ms	2038 s	2038 s	2038 s	2039 s
I		2023 m	2027 m	2028 m	2024 m	2023 ms
II	2016 br	2012 sh	2015 sh	2018 m	2016 sh	2012 m
I		2000 mw	2004 mw	2006 sh	2003 w	2000 sh
II	1990 m	1992 m	1995 m	1992 m	1992 mw	1991 m
I		1983 mw	1984 mw	1982 mw	1982 mw	1983 mw

[a] In hexane, 25 °C, cm^{-1}; v = very, s = strong, m = medium, w = weak. [b] I = $HFeCo_2(CO)_9(CR)$; II = $FeCo_2(CO)_9(HCR)$. [c] Major contribution from II.

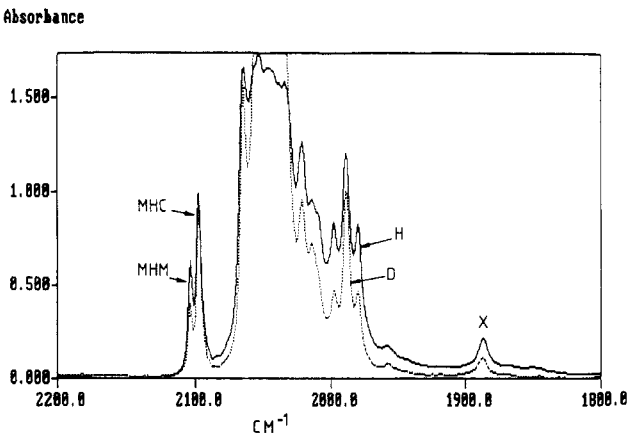

Figure 2. Comparison of the infrared spectra of $FeCo_2(CO)_9$(CHPh) (solid line marked H) and $FeCo_2(CO)_9$(CDPh) (dashed line marked D) in hexanes. X refers to a small impurity of $HFeCo(CO)_{12}$. MHC and MHM refer to the tautomers II and I, respectively.

of the bands to either tautomer I or II by utilizing the H/D isotope effect on reaction 1. It is well-known that if the force constants associated with a hydrogen atom in two different tautomeric forms differ, then an equilibrium isotope effect will exist favoring deuterium in the site with higher force constants, i.e., the C–H–M site in II.[19] The solid and dotted line spectra in Figure 2 correspond to $FeCo_2(CO)_9$(CHPh) and $FeCo_2(CO)_9$(CDPh), respectively. These *carbonyl* bands have been adjusted such that the absorbances of the band at 2099 cm^{-1} match. One immediately notes that the absorbance of the band at 2105 cm^{-1} is greatly reduced relative to that at 2099 cm^{-1} in going from H to D. First, this shows that the two bands result from two different species, namely, I and II. Second the ratio of these two species changes in going from H to D. As the absorption at 2105 cm^{-1} decreases, it is assigned to I, while that at 2099 cm^{-1} is assigned to II. In a similar fashion several other bands can be assigned to one species or the other. Thus, the overall IR spectrum is a superposition of two spectra, each of which is only modestly more complex than that observed for $Co_3(CO)_9CR$, for which four bands are usually observed.[20,21] The results are gathered in Table I.

Corroboration of the assignment comes from an analysis of the magnitude of the isotope effect. By estimating the frequencies associated with the C–H–M and M–H–M interactions, the equilibrium isotope effect can be calculated.

Chart II

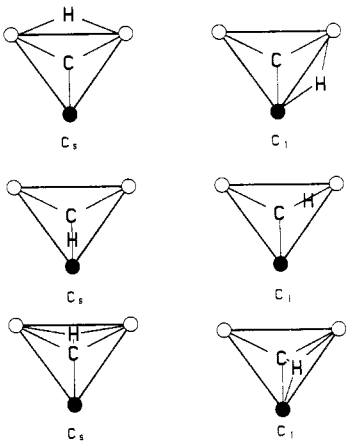

For simplicity, only the highest frequency for each interaction is used. Literature values for closely related systems suggest that 2700 and 1600 cm^{-1} are reasonable frequencies for the C–H–M and M–H–M interactions, respectively.[5] This yields an equilibrium isotope effect of 0.53 favoring deuterium in the C–H–M position, which considering the uncertainty in the frequencies is in excellent agreement with the measured value of 0.67.

The IR data in Table I allow the positioning of the endo hydrogen on I and II to be defined more precisely. Corresponding CO bands in I and II generally differ by 6–10 cm^{-1} with those of II appearing at lower energy. However, the band at 1992 cm^{-1} assigned to II appears to be split into two bands for I (see Figure 2.). This suggests a lower symmetry for I vs II. The ^1H NMR chemical shift suggests an edge bridging M–H–M hydrogen, while the M–H–C hydrogen may be edge or face bridging. The possible arrangements are given in Chart II along with the symmetries. For I to have a lower symmetry than II, I must have an Fe–H–Co edge bridging hydrogen and II must have either an edge bridging Fe–H–C or a face bridging Co_2–H–C. As one Co site has a normal "tilt" angle (Θ) associated with the CO ligands (see above), an edge bridging C–H–Fe hydrogen is favored and Chart I represents the most probable structures of I and II in solution.

Thermodynamic Parameters of the Tautomerization

Equilibrium and Rate Constants. At low temperature the relative intensities of the ^{13}C and ^1H NMR signals indicate II as the more abundant tautomer in toluene (Figure 3 and Table II). Because of the difficulties in accurately integrating different proton resonances,[22] the

(19) Melander, L. *Isotope Effects on Reaction Rates*; Ronald Press, 1960.
(20) Seyferth, D. *Adv. Organomet. Chem.* **1976**, *14*, 97.
(21) Dolby, R. Robinson, B. H. *J. Chem. Soc., Dalton Trans.* **1972**, 2046.
(22) Crabtree, R. H.; Segmuller, B. E.; Uriarte, R. J. *Inorg. Chem.* **1985**, *24*, 1949.

Table II. ^{1}H NMR Spectra for $FeCo_2(CO)_9(CHR)$[a]

	Me		Ph		2,3-$Me_2C_6H_3$		β-napth	
assgnt[b]	−50°C	85°C	−50°C	85°C	−61°C	70°C	−40°C	70°C
M*H*M	−18.15 s		−17.81 s		−17.77 s		−17.76 s	
	[0.5]		[47]		[44]		[42]	
av		−10.42 br		−12.00 br		−11.70 br		−11.30 br
C*H*M	−9.56 s		−8.23 s		−8.16 s		−8.05 s	
	[100]		[100]		[100]		[100]	
Me (II)	2.27 s				0.91 s			
	[300]					1.20 s		
av		2.82 s						
Me, (I)	2.91 s							
	[30]							
Ar			6.5–8.0 m		6.5–7.5 m		6.5–8.5 m	

[a] δ at 300 MHz in $C_6D_5CD_3$. [b] s = singlet, m = multiplet, br = broad; number in brackets = relative area; II = $FeCo_2(CO)_9(HCR)$; I = $HFeCo_2(CO)_9(CR)$.

Table III. Equilibrium Ratios [*K*] for $HFeCo_2(CO)_9CR = FeCo_2(CO)_9(HCR)$

	Me	Ph	3-PhC_6H_4	*t*-BuC_6H_4	β-napth	2,3-$Me_2C_6H_3$
K (NMR)[a]	10 [−50][b]	2.1 [−50][c]			2.4 [−40][c]	2.3 [−40][c]
	8.0 [85][d]	1.5 [85][d]			1.99 [70][d]	1.79 [70][d]
K (IR)[e]	8.83	1.59[f]	1.80	2.37	2.20	2.43
		2.42[g]				
		1.0[h]				
σ[i]		0.0	0.009	−0.197	0.170	−0.303

[a] In toluene. Temperature (°C) in brackets. [b] From integrated Me resonances. [c] From integrated C–H–M and M–H–M resonances. [d] From coalescence chemical shift. [e] In hexane at 25 °C. [f] For $FeCo_2(CO)_9(CHR)$. [g] For $FeCo_2(CO)_9(CDR)$. [h] In toluene at 25 °C. [i] From ref 27.

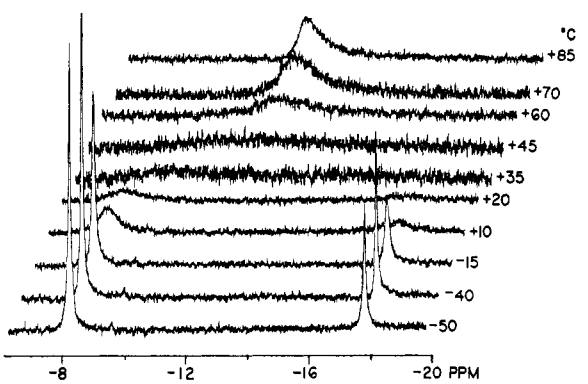

Figure 3. ^{1}H NMR spectrum of $FeCo_2(CO)_9(CHPh)$ in $C_6D_5CD_3$ in the hydride region as a function of temperature.

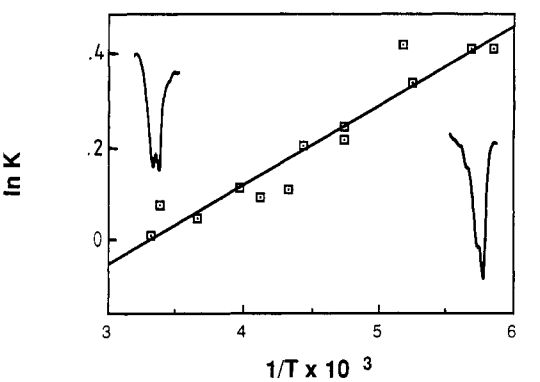

Figure 4. Plot of ln *K*, where $K = A(II)/A(I)$ and *A* = absorbance, as a function of $1/T$ (1/kelvin) for reaction 1 for R = Ph in toluene as a solvent. The absorptions at 2105 and 2099 cm^{-1} for I and II respectively were measured and typical absorptions at 25 and −90 °C are shown as insets. The straight line is a least-squares fit of the data, half of which was obtained decreasing the temperature and half increasing the temperature.

ratio of the integrated signals may contain a systematic error when used as a measure of the equilibrium constant for the tautomerization. The chemical shifts of the coalescence peak and the two individual resonances for I and II at low temperature can also be used to calculate the ratio of II to I in the system at the coalescence temperature.[23] In doing so the temperature variations of the chemical shifts are assumed small. The results are gathered in Table III. Because of the complex NMR behavior it is difficult to obtain a precise measure of the thermodynamic parameters from the NMR data alone. However, these data do suggest that reaction 1 is exothermic.

The fact that some of the CO stretching bands of the two tautomers, I and II, can be resolved means that the equilibrium ratios can be measured directly and independently by IR spectroscopy. This has been done by using the 2099- and 2105-cm^{-1} absorptions as a relative measure of II and I, respectively, and the equilibrium constants are compiled in Table III. In calculating the equilibrium ratio, we have assumed the extinction coefficients for both tautomers are equal. As the IR method has a much smaller intrinsic time constant than the NMR method, it may be used to obtain a more precise measure of the temperature variation of the equilibrium ratio in a system that exhibits fluxionality on the NMR time scale. Again using the 2099- and 2105-cm^{-1} absorptions, measurements of II/I as a function of temperature have been carried out for R = Ph, and the data are presented in Figure 4. The measurements were made in toluene as a solvent, and, hence, the resolution is not as high as in hexane (Figure 2). The thermodynamic parameters calculated from Figure 4 are $\Delta H^\circ = -350 \pm 40$ cal/mol and $\Delta S^\circ = -1.2 \pm 0.2$ eu, where the standard errors of the regression coefficients are given. Measurements were made with both increasing and decreasing temperature. Clearly Figure 4 demonstrates the weak dependence of the ratio of I and II on temperature and the fact that reaction 1 is exothermic.

The IR data also show that there is a solvent effect on the equilibrium ratio of I and II. This has been observed previously for a related system.[6] Comparison of the data

(23) Sandström, J. *Dynamic NMR Spectroscopy*; Academic: New York, 1982.

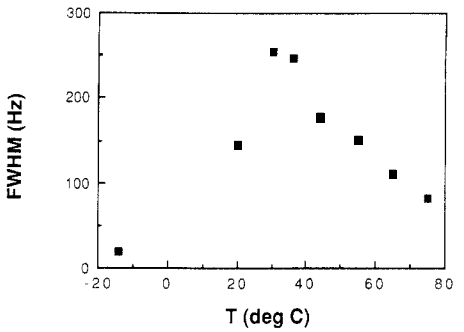

Figure 5. Plot of the broadening (full width at half-maximum) of the major high-field resonance (C–H–M) vs temperature for $FeCo_2(CO)_9(CHMe)$. The temperature of maximum broadening is 33 °C.

Table IV. First-Order Rate Constants for the Reaction $HFeCo_2(CO)_9CR \rightarrow FeCo_2(CO)_9(HCR)$ Determined by ^1H NMR Line Widths as a Function of Temperature[a]

R	10^3k, s^{-1}	T, °C	$\Delta G^{\ddagger}$, kcal/mol
Me	5.96	33	12.66
Ph	6.20	45	13.16
β-napth	5.76	44	13.14
2,3-$Me_2C_6H_3$	5.83	43	13.11

[a] 300 MHz in $C_6D_5CD_3$.

also reveals an apparent systematic error between the NMR and IR methods. For R = Ph, the NMR data requires a equilibrium ratio >1.5 at room temperature, whereas the measured value by IR is ≈1.0. On the other hand, the direction and magnitude of the temperature variation of the equilibrium ratio are crudely the same for both methods. Alternatively, if one assumes $\Delta H^\circ = -350$ cal/mol for the NMR data, one calculates $\Delta S^\circ \approx -0.2$ eu. Hence, despite the discrepancy both methods indicate that reaction 1 is slightly exothermic with a small negative entropy change.

Finally, for completeness the rate constant for the conversion of I to II is obtained at the coalescence temperature by an analysis of the line width as a function of temperature. In Figure 5 an example of such an analysis is presented for the methyl derivative of I/II. At the temperature of maximum broadening, k_f for reaction 1 is given by p_{II}/τ_c where p_{II} is the fraction of tautomer II and $\tau_c = X/2\pi\delta\nu$. In turn $\delta\nu$ is the chemical shift difference between the two resonances, and X is given by $\Delta p = (1/X)[(X^2 - 2)/3]^{3/2}$.[23] The measured rate constants and the corresponding free energies of activation are given in Table IV.

Substituent Effects. NMR measurements have been made on reaction 1 with several different substituents on the capping carbon atom. A set of typical ^1H NMR spectra for the phenyl derivative are shown in Figure 3, and the chemical shift data for the other derivatives are gathered in Table II. The same equilibria plus an additional two have been examined by the IR method, and the equilibrium ratios determined by both methods are gathered in Table III.

The equilibrium ratios for R = Me and Ph in Table III demonstrate that the substituent on the capping carbon has an effect on the equilibrium position of reaction 1. These two equilibrium ratios are displayed in Figure 6 and compared with the data reported earlier for the $Fe_3(CO)_9(CH_3R)$ cluster, R = H[10], Me[24], with the R groups ordered according to size. For R = Me the ratio is an upper limit based on the S/N of the NMR experiment. This

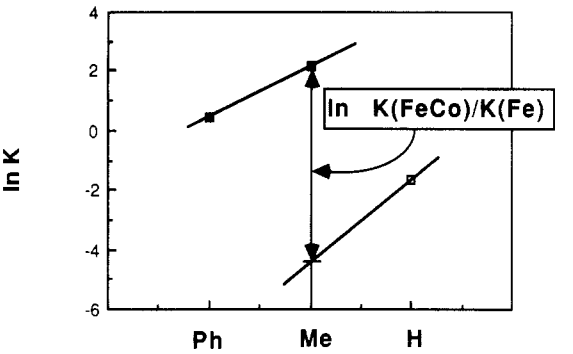

Figure 6. Comparison of the effect of an apical substituent on $Fe_3(CO)_9(CH_3R)$ (open squares) and $FeCo_2(CO)_9(CHR)$ (solid squares, IR data only) at 25 °C. Note that in the former case the value for Me is an upper limit. The difference in the two curves defines the effect of changing metals.

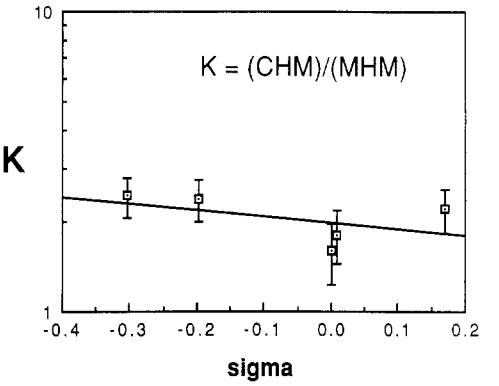

Figure 7. Plot of ln K determined by the IR method (see text) for the reaction $HFeCo_2(CO)_9(CR) = FeCo_2(CO)_9(HCR)$, where R are substituted phenyl groups (see Table III), as a function of the Hammett σ constant. The least-squares fit is ln $K = 2.01 - 1.05\sigma$. A similar plot for the NMR determinations yields ln $K = 1.77 + 0.26\sigma$.

figure demonstrates that in going from the Fe_3H_3 cluster to the $FeCo_2H$ cluter, the C–H–M interaction is promoted by at least 4 kcal/mol in free energy. Hence, Figure 6 expresses the net effect of changing the identity of the transition metal on a chemical process. It is a small but significant change, i.e., a free energy difference of this magnitude can lead to a discrimination factor of 10^3 between two different reaction paths. Note that we have quantitatively measured the effect changing metal character without a changing the exo ligands on the metals themselves.[25] This is an important point simply because exo ligands constitute a large perturbation of the metal and, hence, it is difficult to separate the effect of mixed ligands vs mixed metals on electronic structure.[26]

Figure 6 also shows that the tendency of a substituent to promote a C–H–M interaction decreases in the order H > Me > Ph. There is no obviously simple electronic explanation of this ordering, e.g., there is no correlation with Taft σ^* constants for the substituents. Hence, we examined the change in the equilibrium ratio for phenyl derivatives as the phenyl group itself was modified by substitution. In this way the electronic effect of the capping carbon substituent was varied while keeping the steric interaction with the equatorial CO's approximately constant. The result of a plot of ln K vs the Hammett σ constant for the substituent on the phenyl group[27] is given

(24) Dutta, T. K.; Meng, X.; Vites, J. C.; Fehlner, T. P. *Organometallics* **1987**, *6*, 2191.

(25) The number of endo hydrogens on the two isoelectronic clusters do differ, however.

(26) Chesky, P. T.; Hall, M. B. *Inorg. Chem.* **1981**, *20*, 4419.

(27) Jaffe, H. H. *Chem. Rev.* **1953**, *53*, 191.

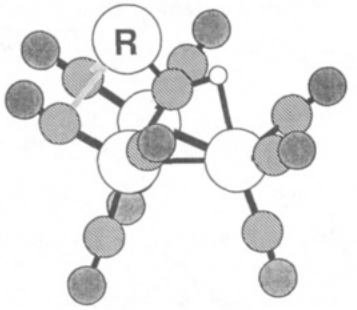

Figure 8. Proposed structure of the tautomer $FeCo_2(CO)_9(HCR)$ showing the steric interaction between R and two of the equatorial CO's of the metal carbonyl framework. A reasonable HCR angle of 113° results in a R–C(CO) distance of 2.5 Å. A similar situation would obtain if the agostic H were placed in a triply bridging position.

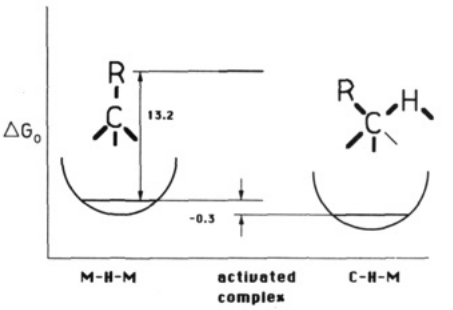

Figure 9. Gibbs free energy diagram for the conversion of I, $HFeCo_2(CO)_9(CPh)$, into II, $FeCo_2(CO)_9(HCPh)$ at 45 °C. The energies are given in kcal/mol.

in Figure 7. Within experimental error there is no change in equilibrium ratio with σ constant and, hence, no measurable electronic effect. Thus, we conclude that the observed order H > Me > Ph is due to a steric effect. As illustrated in Chart I, moving a bridging hydrogen from a M–M edge to a M–C edge causes the R group to move off the pseudo C_3 axis. This prevents the R–C–H angle from becoming too acute while at the same time retaining the known C–H–M geometry.[28] In doing so a repulsive interaction between R and one or more equatorial CO ligands is created (Figure 8) with a consequent decrease in the equilibrium ratio for reaction 1. Hence, the observed effect of the identity of R on reaction 1 results from the steric presence of the exo ligands on the metals and is separable from that due to the change in the metals themselves.

The negative entropy associated with reaction 1, R = Ph, is also consistent with the presence of a significant steric interaction between the phenyl group and the equatorial CO ligands in tautomer II. In going from I to II, M–H–M and C–M interactions are replaced with M–M and C–H–M interactions. The hydrogen-bridged interactions will have relatively high vibrational frequencies (see above) while C–M and M–M vibrational frequencies are in the ranges of 300 and 150 cm^{-1}, respectively.[29] At room temperature the latter will be the dominant contributors to the entropy, and hence, ignoring any other changes, the entropy of II should be larger than that of I and $\Delta S > 0$. In addition, however, in going from I to II a free rotation associated with the phenyl substituent will be frozen out due to the interaction of the phenyl group with the equatorial CO ligands (see Figure 8). For this interaction $\Delta S < 0$, and hence the net entropy change is small as observed.

Discussion

In terms of the cluster–surface analogy, reaction 1 constitutes a model for the interconversion of alkyne and alkene fragments on a trimetal surface site. As shown in Figure 9 the measurements reported here allow us to construct a complete free energy diagram for this reaction at a single temperature. In terms of a potential model for a catalytic process, this is exactly the type of diagram one expects to observe, i.e., potential wells of stable structures of nearly equal energy connected by a low energy barrier. A small perturbation of the system caused by temperature, concentration, metal, etc., can thus result in an efficient conversion of one species into the other.

The small free energy change in the I = II equilibrium might be taken to imply that little change in the nature of the hydrocarbon fragment takes place in going from I to II, i.e., the interconversion is no more significant than an ordinary fluxional process involving hydrogen atoms. However, two observations suggest that the hydrocarbyl fragment in I is essentially different from that in II. First, in going from I to II the ^{13}C chemical shift changes from a value typical of an alkyne fragment to one typical of an alkene fragment. Second, we have pointed out in earlier work[8] that increasing the number of C–H–M interactions in a capped trimetal cluster system results in a large decrease in the s character of the capping atom as measured by the capping atom–exo hydrogen coupling constant. Both these observations suggest that the hydrocarbyl fragment in I is a real alkyne and that in II is a real alkene.

Why, then, is only a small overall energy change observed? There must be a large change in the electronic structure of the trimetal carbonyl fragment that balances the change in the carbon fragment. A comparison of the IR spectra of I and II supports this conclusion. In moving the endo hydrogen from a M–M to M–C bridging position the CO frequency of the symmetrical in-phase band near 2100 cm^{-1} goes down by about 7 cm^{-1}. This difference, caused by the "simple" rearrangement of the endo hydrogen, is 10% of that observed in changing the overall cluster charge by one by, for example, deprotonation. Hence, it appears that the large change in the hydrocarbyl fragment is balanced by a similarly large change in the metal carbonyl fragment. Clearly, it is the ability of the metal carbonyl fragment to accommodate itself to a variety of bonding situations that permits the nearly isoenergetic interconversion of I and II.

It is interesting to note that, on the basis of the IR frequencies the alkyne fragment plus a M–H–M hydrogen appears to withdraw more negative charge from the metal carbonyl fragment than does the alkene fragment. We have argued previously[15,30] that transfer of negative charge to a carbon atom is one driving force for the reduction of a hydrocarbyl fragment on a boron (and, by analogy, metal) framework. Clearly the distribution of electronic charge between the metal framework and the hydrocarbyl fragment is also important here.

Conclusions

Although the chemical consequences of changing metal identity in metal clusters is of great interest,[31] the change is such a subtle one that only sensitive measurements

(28) Beno, M. A.; Williams, J. M.; Tachikawa, M.; Muetterties, E. L. *J. Am. Chem. Soc.* **1981**, *103*, 1485.
(29) See, for example: Andrews, J. R.; Kettle, S. F. A.; Powell, D. B.; Sheppard, N. *Inorg. Chem.* **1982**, *21*, 2874.
(30) DeKock, R. L.; Fehlner, T. P.; Housecroft, C. E.; Lubben, T.; Wade, K. *Inorg. Chem.* **1982**, *21*, 25.
(31) Sinfelt, J. H. *Acc. Chem. Res.* **1977**, *10*, 15.

reveal it. Often even calculational methods fail to reveal significant changes in electronic structure for mixed-metal systems.[32] Kinetic measurements, on the other hand, allow the greater reactivity of Ru over Os with respect to reductive elimination H_2 from trimetal clusters to be conclusively demonstrated.[33] Here we have used the position of equilibrium as a measure of the tendency of the trimetal base to facilitate the transfer of hydrogen to an attached carbon atom. Going from Fe to Co promotes the formation of C–H bonding at the expense of M–H bonding. The work also demonstrates that the exo ligands of the discrete cluster that are not present on a surface site can play a role. Here the observed effect is apparently steric in nature, but certainly there is an electronic role as well. By comparing clusters in which the exo ligands on the metals are identical, one expects that the significant electronic perturbation of the metal centers by these ligands will largely cancel in the comparison. Thus, we expect that the behavior of Co with respect to Fe in these discrete trimetal carbonyl clusters can be taken as a qualitative measure of the behavior of Co with respect to Fe at a trimetal surface site on a bulk metal.

Experimental Section

General Procedures. All reactions were carried out with standard Schlenk techniques.[34] Solvents were dried (toluene over anhydrous $MgSO_4$, THF over KOH pellets, hexane over molecular sieve), degassed, and distilled (from sodium benzophenone ketyl) before use. The following reagents were used as received unless otherwise noted: C_6D_6, $C_6D_5CD_3$, D_3PO_4 (Aldrich); $AlCl_3$, H_3PO_4 (Fisher); $Na_2Fe(CO)_4 \cdot {}^3/_2C_4H_4O_2$ (Alfa); $Co_2(CO)_8$ (Strem); $^{13}CCl_4$, 99+% (Merck). Columns were prepared with Fisher 60–200 mesh silica gel.

Routine ^1H NMR spectra were obtained on a Magnachem A-200 FT spectrometer, and variable-temperature ^1H and ^{13}C NMR spectra were obtained on a Nicolet NB 300 or General Electric GN 300 FT spectrometers. Mass spectra were obtained on a Finnigan MAT 8450 mass spectrometer. IR spectra were recorded on Perkin-Elmer 1420 grading and IBM IR/32 FT spectrometers. Variable-temperature IR measurements were carried out with the former instrument utilizing a Specac P/N 21.500 cell with temperature control (ARIES, Concord, MA). Chemical shifts are reported as follows: ^1H, residual signal of C_6D_6 δ 7.15; ^{13}C, residual signal of C_6D_6 δ 128.0.

Preparation of $FeCo_2(CO)_9(CHR)$. The preparation of the $FeCo_2(CO)_9(CHR)$ clusters was carried out by using the literature reactions[12,21,35,36] with the indicated modifications (eq 2–4).

$$Co_2(CO)_8 + CCl_4 \xrightarrow[4\text{–}5\ h]{50\ ^\circ C} \underset{30\%}{Co_3(CO)_9CCl} + CO + CoCl_2 \quad (2)$$

$$Co_3(CO)_9CCl + C_6H_6 \xrightarrow[\substack{AlCl_3,4\text{–}5\ h\\ THF,\ reflux}]{70\ ^\circ C} \underset{50\%}{Co_3(CO)_9CPh} + HCl \quad (3)$$

$$Co_3(CO)_9CPh + [Fe(CO)_4]^{2-} \xrightarrow[2\ h]{} [FeCo_2(CO)_9CPh]^-$$

$$[FeCo_2(CO)_9CPh]^- + H_3PO_4 \rightarrow \underset{30\%}{FeCo_2(CO)_9(CHPh)} \quad (4)$$

Isolated yields are as indicated. The reaction scale was 0.5 g (1.5 mMol) of $Co_2(CO)_8$ with excess of CCl_4. The solvent in reaction 2 was removed under vacuum, and the product dissolved. The mixture was then filtered through Celite and washed alternately with 10-mL portions of 10% HCl and water until the aqueous layer is colorless. The hexane solution was dried over $MgSO_4$, and the solvent removed under vacuum, yielding purple crystals. After removal of the solvent under vacuum, the product of reaction 3 was dissolved in hexane, filtered through Celite, and chromatographed on silica gel. The brown band eluding with hexane yields brown crystals. The anionic product of reaction 4 was extracted three times with 10-mL portions of 40% H_3PO_4 plus 10–15 mL of hexane. The combined and concentrated extracts were placed on a silica gel column and washed with hexane. The red band remaining at the origin was removed with methanol. On removing the methanol and reacidfying in the same manner, the final product was isolated as brown crystals from hexane. The final product was stored under 1 atm of CO to retard decomposition into $Co_3(CO)_9CR$ and $HFeCo_3(CO)_{12}$.

For R = Me, $MeCCl_3$ was used in place of CCl_4 to produce $Co_3(CO)_9CMe$ directly.[37] For the preparation of $FeCo_2(CO)_9$(CDPh) 40% D_3PO_4 in D_2O was used in the last step. For the ^{13}C-labeled compound reaction 2 was carried out with 1.0 g of 99.9% $^{13}CCl_4$ in 10–15 mL of toluene with a reaction time of 24 h. Since only half of the starting material reacts in 2, this step was repeated to increase the overall yield.

Products were characterized by mass spectrometry {R = 3-PhC_6H_4 (p^+ = 592, 9 CO); R = t-BuC_6H_4 (p^+ = 574, 9 CO); R = $C_{10}H_7$ (p^+ = 566, 9 CO); R = 2,3-$Me_2C_6H_3$ (p^+ = 544, 9 CO)}, IR (Table I), and in some cases ^1H NMR (Table II). Apparently $Co_3(CO)_9CR$, R = t-BuC_6H_4, has not been reported (p^+ = 576, 9 CO; IR (hexane, cm^{-1}) 2101 m, 2056 vs, 2038 s, 2021 m, 1981 w).

Acknowledgment. The support of the National Science Foundation is gratefully acknowledged, as is the aid of D. R. Schifferl with the NMR experiments.

(32) Harris, S.; Blohm, M. L.; Gladfelter, W. L. *Inorg. Chem.* **1989**, *28*, 2290.
(33) Keister, J. B.; Onyeso, C. C. O. *Organometallics* **1988**, *7*, 2364.
(34) Shriver, D. R.; Drezdzon, M. A. *The Manipulation of Air Sensitive Compounds*, 2nd ed.; Wiley-Interscience: New York, 1986.
(35) Palyi, G.; Piacenti, F.; Marko, L. *Inorg. Chim. Acta, Rev.* **1970**, *4*, 104.
(36) Nestle, M. O.; Hallgen, J. E.; Seyferth, D. *Inorg. Synth.* **1980**, *20*, 234.
(37) Nivert, Cl. L.; Williams, G. H.; Seyferth, D. *Inorg. Synth.* **1980**, *20*, 226.